LETTER Communicated by Tassilo von der Twer

Novel Perceptually Uniform Chromatic Space

María da Fonseca
mariadafon@gmail.com
Inés Samengo
ines.samengo@gmail.com
Medical Physics Department, Instituto Balseiro and Centro Atómico Bariloche, 8400 San Carlos de Bariloche, Argentina

Chromatically perceptive observers are endowed with a sense of similarity between colors. For example, two shades of green that are only slightly discriminable are perceived as similar, whereas other pairs of colors, for example, blue and yellow, typically elicit markedly different sensations. The notion of similarity need not be shared by different observers. Dichromat and trichromat subjects perceive colors differently, and two dichromats (or two trichromats, for that matter) may judge chromatic differences inconsistently. Moreover, there is ample evidence that different animal species sense colors diversely. To capture the subjective metric of color perception, here we construct a notion of distance in color space based on the physiology of the retina, and is thereby individually tailored for different observers. By applying the Fisher metric to an analytical model of color representation, we construct a notion of distance that reproduces behavioral experiments of classical discrimination tasks. We then derive a coordinate transformation that defines a new chromatic space in which the Euclidean distance between any two colors is equal to the perceptual distance, as seen by one individual subject, endowed with an arbitrary number of color-sensitive photoreceptors, each with arbitrary absorption probability curves and appearing in arbitrary proportions.

When we open our eyes, most of us see a colorful world. The chromatic sensations we experience depend on many factors. Here we discuss the role of one such factor: the spectral power density of the light entering through our pupils. The space of all possible spectra is infinite-dimensional. However, observers with three types of cones are oblivious to most dimensions, perceiving only a subspace of three chromatic dimensions. The act of observing, hence, is mathematically equivalent to projecting the space of all light spectra onto a three-dimensional subspace (Koenderink & Van Doorn, 2003). Classical color-matching experiments (Wyszecki & Stiles, 2000) allow us to identify the subspace that one particular observer is sensitive to.

Neural Computation **30, 1612–1623** (2018)
doi:10.1162/neco_a_01073

The retina of most human observers is endowed with three types of cones, sensitive to *S* (short), *M* (medium), and *L* (long) wavelengths. The probability that a cone of each type captures a photon of wavelength λ defines three curves $h_S(\lambda)$, $h_M(\lambda)$, $h_L(\lambda)$: the so-called cone fundamentals (Stockman & Brainard, 2009). In most observers, these curves peak at 442.1 nm, 542.8 nm, and 568.2 nm, respectively, and partially overlap with each other. Some subjects possess anomalous color-sensitive absorption proteins, giving rise to altered absorption probabilities peaking at slightly different wavelenghts, thereby producing anomalous trichromacy. Roughly 95% of humans are trichromats, and about 3% of them have anomalous trichromacy. Approximately 5% of humans are dichromats (endowed with two types of cones), and a very small fraction of the population is not color sensitive at all. In addition, there might be a few rare examples of tetrachromats (Jordan, Deeb, Bosten, & Mollon, 2010), endowed with mosaic retinas that include both normal and anomalous light-sensitive receptors. Finally, color sensitivity is determined not only by the number of types of color-sensitive receptors but also by their relative proportions. In fact, humans display a remarkable variability in the relative proportion of *M* and *L* cones (Hofer, Carroll, Neitz, Neitz, & Williams, 2003; Roorda & Williams, 1999).

The overwhelming majority of standard trichromats has directed all previous attempts to construct color spaces toward universal three-dimensional representations, that is, representations that are suited for no particular subject but, rather, for some ideal "standard trichromat observer." The Munsell color system was introduced in 1910 and contains three orthogonal axes: hue, lightness, and chroma (Landa & Fairchild, 2005; Munsell, 1912). The CIE 1931 *XYZ* color space was created by the Commission Internationale de l'Éclairage and emerges naturally from color-matching experiments (Malacara, 2011; Wyszecki & Stiles, 2000). Its reduction to a two-dimensional space *xy* retains only the hue and the chroma, disregarding a third coordinate that approximates the apparent luminosity. In 1984, after the discovery of the opponent-color characteristics in the lateral geniculate nuclei, Derrington, Krauskopf, and Lennie (1984) introduced the DKL space. Its axes represent the opponency between the output of cones. All these spaces, although adequate to represent some characteristics of chromatic stimuli, had the rather inconvenient property of being perceptually inhomogeneous: observers were able to make fine discriminations between neighboring colors in certain regions of color space but not in others. The Euclidean distance between two neighboring colors, hence, was not representative of their behavioral discriminability. New representations of colors were therefore introduced, aiming at obtaining a space that would better represent the accuracy observed in discrimination experiments. Several attempts were made to define a so-called uniform-chromaticity scale diagram, all defined as nonlinear transformations of CIE 1931 *XYZ* color space. In 1944, MacAdam (1944) attempted to reach perceptual uniformity, proposing a nonlinear geodesic transformation based

on experimental data. His proposal was adopted by the CIE in 1960 as a standard uniform color space (UCS) diagram, named the CIE 1960 UCS diagram, with coordinates Luv (Wyszecki & Stiles, 2000). In 1976, the CIE applied two modifications to this diagram. First, a coordinate transformation $Luv \to L'u'v'$ was introduced to define the CIE 1976 UCS diagram. Then, after some other modifications, an additional transformation led to the CIE Luv space, with coordinates $L^*u^*v^*$ (Wyszecki & Stiles, 2000). Also in 1976, the CIE defined a new space called CIE Lab that attempted to approximate both color uniformity and color opponency (Malacara, 2011). Each of these alternatives had its own advantages and disadvantages. None of them, however, was tailored to individual observers. Moreover, none of them was truly perceptually uniform for the standard trichromat, so in a way, they all failed to accomplish the purpose that inspired their definition.

Our aim is to construct a space that is perceptually uniform, that is, a space in which the colors that are discriminated with equal accuracy are represented by points located at equal distances. The first requirement to accomplish this task is to construct two notions of distance: (1) a notion of perceptual distance between colors, based on the discrimination ability of one individual observer, and (2) a notion of mathematical distance in the space representing colors. Here we search for a perceptually uniform space that reveals color differences in an intuitive fashion, so we take the mathematical notion of distance of (point 2) as the usual Euclidean distance. If we begin representing colors using any of the well-known color coordinate systems, by performing experiments, we will give rise to a notion of distance 1 that will most likely not coincide with the Euclidean notion of distance 2. The second step in this endeavor is hence to define a change of coordinates from the original coordinate system to some new color space that maps the notion of distance 1 into Euclidean distance 2, as done below.

Notion 1 must be based on perceptual experiments and is expected to vary from observer to observer. Many such experiments have been performed, using different paradigms to evaluate color discriminability (Holtsmark, 1969; MacAdam, 1942; Pokorny & Smith, 1970; Wright & Pitt, 1934). All paradigms are based on the fact that visual sharpness has finite acuity, so if two colors are sufficiently close to one another, an observer will not be able to perceive them as different. Experiments, hence, aimed at determining the set of colors that were not discriminated from one given color. The surface defined as the outer border of such a region contains the closest set of colors that are discriminated from the one at the center. Building a notion of distance using criterion 1 boils down to noticing that from a perceptual point of view, it makes sense to regard the colors on this surface as all lying at the same distance from the one at the center. Interestingly, experiments showed that such surfaces were always ellipsoids, implying that a metric-based notion of distance is applicable. In other words, the notion of distance that emerges from discrimination experiments may be obtained as the norm of a scalar product defined in color space. For each observer, then, we need

to construct the second-rank tensor defining the scalar product. The eigenvectors of the tensor evaluated at each point correspond to the directions of the principal axes of the measured ellipsoid, and the associated eigenvalues determine their lengths. Within this framework, the recipe to obtain notion 1 of distance required above is:

1. Perform a discrimination experiment on a finite set of points $\mathbf{x}$ scattered throughout the space of colors and determine, for each $\mathbf{x}$, the ellipsoid around it containing the colors that are not discriminated from $\mathbf{x}$.
2. Calculate the directions and lengths of the principal axes of all the measured ellipsoids.
3. In each point $\mathbf{x}$ of color space, define a metric tensor $J(\mathbf{x})$ as the 3×3 matrix whose eigenvectors and eigenvalues coincide with the directions and lengths calculated in the second step.
4. Define a notion of distance between two neighboring colors $\mathbf{x}$ and $\mathbf{x} + \mathrm{d}\mathbf{x}$ as $\mathrm{dist} = \sqrt{\mathrm{d}\mathbf{x}^t J(\mathbf{x}) \mathrm{d}\mathbf{x}}$, where the superscript t indicates vector transposition.
5. Define the distance between two remote colors $\mathbf{x}_a$ and $\mathbf{x}_b$ along a path connecting them as the sum of the differential distances of the line elements along the path.

To obtain a perceptually uniform space, we need to find a change of coordinates $\mathbf{x}' = \mathbf{F}(\mathbf{x})$ that transforms the metric tensor $J(\mathbf{x})$ into the identity matrix, that is, $J'(\mathbf{x}') = \mathbb{1}$. When the scalar product of a given space is represented by the identity matrix, distances coincide with our intuitive Euclidean notion. As a result, in the transformed space, all the minimally discriminable ellipsoids become spheres, and all spheres have the same size. The transformed tensor $J'(\mathbf{x}')$ is obtained from the original tensor $J(\mathbf{x})$ by using the relation $J(\mathbf{x}) = C^t\, J'(\mathbf{x}')\, C$, where C is the Jacobian matrix, that is, $C_{ij} = \partial x'_i / \partial x_j$.

In this letter, instead of gathering experimental data as stated in step 1 of the recipe listed above, we define the perceptual metric using the analytical approach introduced by da Fonseca and Samengo (2016), based on the notion of Fisher information (Amari & Nagaoka, 2000). The theory was developed from first principles, based on the statistics of photon absorption (Zhaoping, Geisler, & May, 2011), and the derived metric tensor closely reproduces the discrimination experiments performed by observers endowed with retinas of different composition. This same metric tensor is employed here, since it allows us to describe observers with arbitrary retinas with analytical tools, and it has proven to reproduce previous experimental data for a variety of observers (da Fonseca & Samengo, 2016; Zhaoping et al., 2011).

Within this framework, the natural coordinates to describe the color with which a light spectrum $E(\lambda)$ is perceived are α_S, α_M, and α_L, defined as

$$\alpha_i = \beta_i \int_0^{+\infty} E(\lambda)\, h_i(\lambda)\, \mathrm{d}\lambda.$$

Here, the coefficients β_i represent the proportion of cones of type i of the observer under consideration. For dichromat observers, one of the β_i vanishes, whereas in the case of tetrachromats, an additional type of photoreceptor β_a and its associated absorption curve $h_a(\lambda)$ are used to define a four-dimensional chromatic space. Notice that the same spectrum may be assigned different color coordinates $\alpha_S, \alpha_M, \alpha_L$ by observers with different retinal compositions, or with different absorption curves.

The metric tensor derived by da Fonseca and Samengo (2016) is the Fisher matrix:

$$J(\alpha_S, \alpha_M, \alpha_L) = \begin{pmatrix} 1/\alpha_S & 0 & 0 \\ 0 & 1/\alpha_M & 0 \\ 0 & 0 & 1/\alpha_L \end{pmatrix}.$$

The mathematical formalism from which this metric tensor emerges guarantees that the distance between any two neighboring colors is, by construction, inversely related to the perceptual discrimination error of an ideal observer interpreting the absorbed photons, as stated by the Cramér-Rao bound (Cramér, 1946). In principle, a real subject need not be an ideal observer, and yet the theory is able to capture 87% of the experimental variability of real observers, implying that color perception is close to optimal (da Fonseca & Samengo, 2016).

Finding a perceptually uniform space, hence, reduces to finding the coordinate transformation $\mathbf{x}' = \mathbf{F}(\alpha)$ that solves the equation

$$\mathbb{1} = C^t\, J(\alpha)\, C.$$

The solution to this system is

$$x'_i = 2\sqrt{\alpha_i} + \mu_i,$$

where the μ_i are arbitrary integration constants, here taken as zero in order for complete darkness to be represented by $\mathbf{x}' = (0, 0, 0)$. In Figure 1, several surfaces of constant illumination are displayed, where illumination is defined as $\alpha_S + \alpha_M + \alpha_L = (x'_S)^2 + (x'_M)^2 + (x'_L)^2 = \text{const}$. As the value of the constant is increased, the spherical surface moves outward, and colors are perceived as brighter. The surface is included in the octant where all x'_i are nonnegative.

Only a limited portion of each surface appears painted, since not all perceived colors can be obtained on a standard computer monitor. More saturated colors should appear in the regions displayed in gray, but those cannot

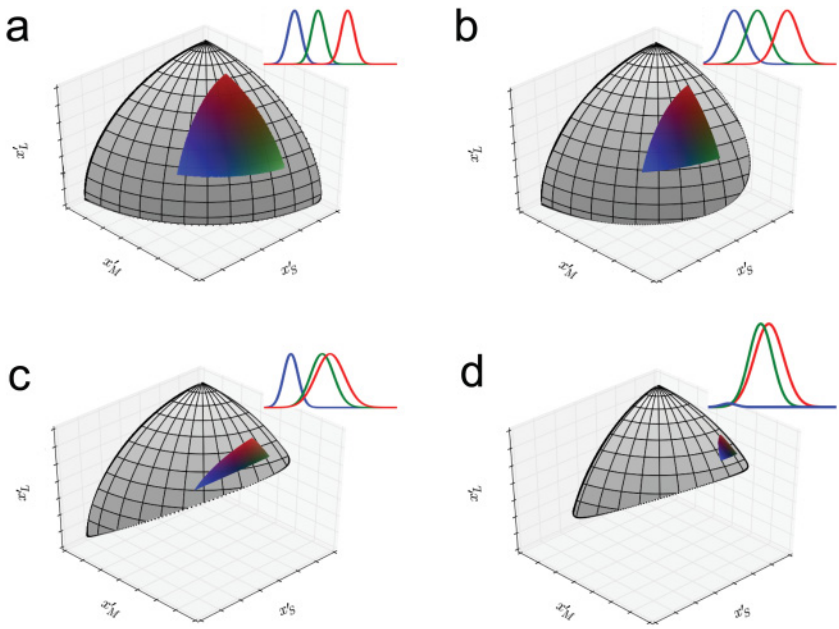

Figure 1: Perceptually uniform space. Surface defined by $\alpha_S + \alpha_M + \alpha_L = (x'_S)^2 + (x'_M)^2 + (x'_L)^2 = \text{const}$. The triangular colored region represents the portion of the surface that can be represented by LED monitors. The curves $h_i(\lambda)$ are modeled as $e^{-(\lambda-\lambda_i)^2/\sigma_i^2}$. Insets: absorption curves, with total height proportional to the fraction β_i of cones of each type. (a) Observer with absorption probabilities similar to the ones reported for the shallow-water fish (Atick, 1992), with $\lambda_S = 455$ nm, $\lambda_M = 530$ nm, $\lambda_L = 625$ nm, and $\sigma_i = 30$ nm, for all i. $\beta_S = \beta_M = \beta_L = 1/3$. (b) Same as in panel a but with widths $\sigma_i = 50$ nm. (c) Observer with absorption probabilities of standard human trichromats (Stockman & Brainard, 2009), with $\lambda_S = 442$ nm, $\lambda_M = 543$ nm, $\lambda_L = 568$ nm, $\sigma_S = 32.96$ nm, $\sigma_M = 52.8$ nm, $\sigma_L = 64.76$ nm, and $\beta_S = \beta_M = \beta_L = 1/3$. (d) Same as in panel c but with more realistic retinal composition: $\beta_S = 0.02$, $\beta_M = \beta_L = 0.49$.

be generated mixing the broad spectra of LEDs. This limitation of computer screens explains why the colors of visual scenes typically appear more vivid when viewed naturally and why virtual museums of the visual arts miss part of the chromatic intensity of real museums. To color the surface, the monitor is instructed to activate its three LEDs with such intensities as to produce, for each of the observers, a spectrum whose $\mathbf{x}'$ coordinates coincide with the location of the point. Different panels correspond to observers endowed with retinas of different composition and physiology. In the four displayed panels, two of the three outer edges of each surface correspond to the colors of the rainbow, which are maximally saturated. The third edge

corresponds to the set of purples (the transition from red to blue), which although not in the rainbow, are still maximally saturated.

In Figure 1a, we see the perceptually uniform color space of a shallow-water fish endowed with three types of photoreceptors (Atick, 1992). For illustration purposes, we scaled the width of the absorption curves (see the inset) to be narrow and thus obtained curves $h_i(\lambda)$ overlapping only minimally with each other. Nonoverlapping absorption curves may be activated independently, resulting in colors with intense hue. For these observers, the accessible space almost coincides with the whole octant of positive $\mathbf{x}'$ values. Monochromatic light sources that activate a single type of cone are located at the corner of this space, whereas sources activating only two of the three types are on the coordinate planes.

In Figure 1b, we analyze a hypothetical observer with absorption curves that peak at the same value as the ones in panel a but with expanded widths, thereby increasing the overlap between the curves. Hence, the activity of different types of cones tends to be correlated. As a consequence, the accessible space shrinks, and its outer border becomes more rounded. In particular, it is now no longer possible to activate the medium-wavelength photoreceptor without activating simultaneously at least one of the other two. No light spectrum exists that exclusively activates M cones, and, therefore, the region of space corresponding to large x'_M is no longer reachable.

Comparing Figures 1a and 1b, we see that the size of the colored region diminishes. Since this space is perceptually uniform, a reduction of the central triangle implies that the colors that can be constructed from a standard computer screen are perceived as all more similar to one another and, at the same time, more different from the maximally saturated colors lying along the outer border. Correlated cone activity produces screen colors to be perceived with less saturation, that is, more grayish, or whiteish. They are therefore not as easy to differentiate. Hence, the central colored triangular region shrinks. In addition, the light spectra that induce maximally saturated percepts in Figure 1b have more extreme properties than the ones producing the same effect in Figure 1a. In order for the observer in Figure 1b to perceive maximally saturated colors, monochromatic light beams that move farther into the ultraviolet or the infrared edges are required to avoid the simultaneous activation of the three types of photoreceptors. In addition, the intensity of the source must be increased enormously to compensate for the sharp decrease of absorption probabilities on the outer borders of the visible spectrum. Hence, the spectra lying on the coordinate planes of Figure 1b contain more extreme wavelengths and intensities than the ones for Figure 1a. It is therefore natural that such spectra are located farther away from anything that a computer screen can produce.

In Figure 1c, we test absorption curves $h_i(\lambda)$ that correspond to standard human trichromats (inset). The most important difference with the case of the shallow-water fish is that the long-wavelength probability is now shifted toward shorter wavelengths, overlapping the medium-wavelength

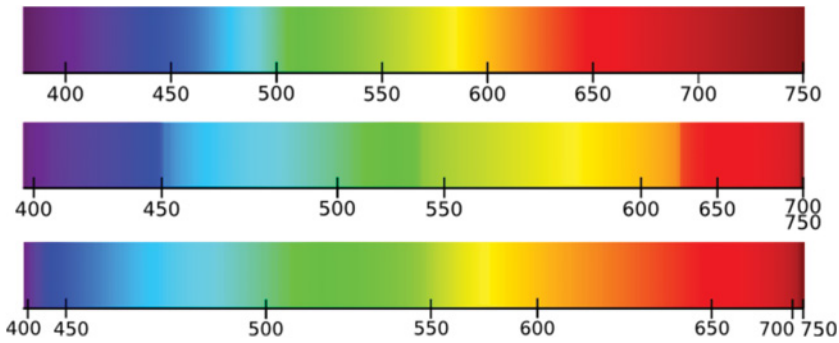

Figure 2: Comparison between different chromatic scales of monochromatic light. The colors are displayed only for orientation purposes. They do not represent the true sensations induced by monochromatic beams, since ordinary LED screens and printers cannot produce saturated colors. (Top) Color palette that varies linearly with wavelength. (Middle) Color palette of perceptually uniform hues for the shallow-water fish of Figure 1a. (Bottom) Color palette of perceptually uniform hues for the human observer of Figure 1d.

curve much more than before. The strong correlation between M and L cones shrinks the accessible space even further, mainly restricting it to the region $x'_L \geq x'_M$. In Figure 1d, we see the perceptually uniform space for a human that has a much larger proportion of M and L cones than of S cones, as is usually the case.

If we vary the wavelength λ of a monochromatic beam in steps of constant $d\lambda$, from the perceptual point of view, the colors that we obtain are not equidistant, as implied by the nonconstant separation between the consecutive dots that conform the outer border of the gray surfaces of Figures 1a to 1d. That is, sometimes an increment in $d\lambda$ results in a color that is clearly discriminable from the previous one, and sometimes not. Varying the wavelength at uniform intervals means to transverse a path along the perceptually uniform space at a nonconstant velocity. Conversely, we could imagine traversing that same path at constant speed and constructing a new palette from the colors that we encounter along our perceptually equidistant journey. In Figure 2, we compare the scales thus obtained for the shallow-water fish (middle stripe) and the human observer (bottom), with the original wavelength-based scale (top).

We observe that for the human observer, the perceptually uniform scale expands the zones corresponding to cyan and orange and contracts the blue and red stripes. The expanded regions result from the high sensitivity to variations in the number of activated cones in the regions where S and M curves overlap or where the M and L curves overlap. Precisely in these zones, the slopes of the activation curves are maximal. In contrast,

the human palette is contracted, implying a loss of sensitivity, around the maxima of the *S*, *M*, and *L* activation curves.

The metric tensor of a perceptually uniform space is represented by the identity matrix, and therefore the curvature vanishes in every point. In 1943, Silberstein (1943) demonstrated that the curvature of the CIE 1931 *xy* chromatic space was significantly different from zero. Since the curvature is an invariant, his result implied that there is no coordinate transformation, no matter whether linear or nonlinear, that can take the *xy* chromatic space to another perceptually uniform space. This conclusion discouraged scientists from searching spaces that were rigorously perceptually uniform' and their efforts focused on more pragmatic approaches. Indeed, scientists became content if only approximately uniform spaces were found. Silberstein's conclusion, however, holds only for the CIE *xy* chromatic space, which is two-dimensional. If such a space is interpreted as a submanifold of a higher-dimensional space, nothing prevents the larger space from being truly perceptually uniform and, at the same time, the submanifold to be curved. The perceptually uniform space introduced here, in fact, is three-dimensional, and it contains different copies of the CIE *xy* space as curved submanifolds, one copy for each possible luminosity level.

In summary, here we offer a perceptually uniform space that, as illustrated by Figures 1 and 2, allows individual observers to represent colors in such a way that the Euclidean distance between pairs of colors coincides with their perceptual distance. Colors viewed by observers with arbitrary retinal compositions can be described, including observers carrying either more or fewer than three types of color-sensitive photoreceptors or even with anomalous absorption curves. This observer-dependent behavior contrasts with previous colorimetric attempts to construct perceptually uniform color spaces designed for an average observer. Our study, however, is not the first to propose a new color space that is individually tailored for each subject. Other approaches have taken the lead in this matter, although their aim was somewhat different from ours: their goal was to derive the way in which the nervous system should internally encode stimuli in order to operate with optimal representations in terms of either minimal mean square error (MacLeod, 2003; MacLeod & von der Twer, 2003; von der Twer & MacLeod, 2001) or of maximal information transfer between the external signal and neuronal activity (Laparra, Jiménez, Camps, & Malo, 2012; Laparra & Malo, 2015). In other words, they worked out the computational consequences of an optimality hypothesis. Their new stimulus space was obtained by applying a nonlinear input-output transformation to the coordinates defining the external signal, and the nonlinearity was chosen by taking into account the probability distribution with which different stimuli appear in nature (Bell & Sejnowski, 1995; Laughlin, 1981, 1983; Srinivasan, Laughlin, & Dubs, 1982) and the noise that is inherent to neuronal activity (Laparra et al., 2012; Laparra & Malo, 2015; MacLeod, 2003; MacLeod & von der Twer, 2003; von der Twer & MacLeod, 2001). As a result, they obtained a

set of uniformly discriminable stimuli at the output, in the same spirit as the theory derived in this letter. The difference between our analysis and previous studies is that our theory is rooted in (1) the very first stage of visual processing, that is, photon absorption alone, and (2) the Fisher information geometry derived from photoreceptor physiology, with no reference to the statistics of natural stimuli. The first point can be viewed as good and bad news. The good news is that just the very first stage of photon processing can explain a large amount of the variance in the behavioral data of color discrimination (da Fonseca & Samengo, 2016). Moreover, the simplicity of the noise model, based on the independent and Poissonian activation of the *S*, *M*, and *L* signals, allows us to derive the uniform color space analytically. The bad news is that the model neglects many processing stages taking place downstream, which are known to exist, as, for example, context-dependent adaptation of neuronal responses, decomposition in achromatic and opponent chromatic channels, and nonlinear saturation of cellular signals (Laparra et al., 2012; Laparra & Malo, 2015; Laparra, Muñoz, & Malo, 2010; Malo & Laparra, 2010; von der Twer & MacLeod, 2001). The second point however, offers a rigorous and systematic method that may be applied to other noise models with more biological detail, as has been done in the context of texture (Berardino, Laparra, Ballé, & Simoncelli, 2017). We hope that this methodology inspires new studies, including other relevant features of the image, as spatial structure, contrast, and texture, and also other computations performed throughout the visual pathway.

Acknowledgments

We thank Nicolás Vattuone for his insightful comments and help. We also thank Federico Clavero for calibrating standard computer screens in order to produce the accurate coloring of Figure 1. This work was supported by Consejo Nacional de Investigaciones Científicas y Técnicas, Agencia Nacional de Promoción Científica y Tecnológica, Universidad Nacional de Cuyo, and Comisión Nacional de Energía Atómica.

References

Amari, S. I., & Nagaoka, H. (2000). *Methods in information geometry*. Oxford: Oxford University Press.

Atick, J. J. (1992). Could information theory provide an ecological theory of sensory perception? *Network: Computation in Neural Systems*, *3*(2), 213–251.

Bell, A. J., & Sejnowski, A. T. (1995). An information-maximization approach to blind separation and blind deconvolution. *Neural Computation*, *7*(6), 1129–1159.

Berardino, A., Laparra, V., Ballé, J., & Simoncelli, E. (2017). Eigen-distortions of hierarchical representations. In I. Guyon, U. V. Luxburg, S. Bengio, H. Wallach,

R. Fergus, S. Vishwanathan, & R. Garnett (Eds.), *Advances in neural information processing systems, 30* (pp. 3533–3542). Red Hook, NY: Curran.

Cramér, H. (1946). A contribution to the theory of statistical estimation. *Scandinavian Actuarial Journal*, *1946*(1), 458–463.

da Fonseca, M., & Samengo, I. (2016). Derivation of human chromatic discrimination ability from an information-theoretical notion of distance in color space. *Neural Computation*, *28*(12), 2628–2655.

Derrington, A. M., Krauskopf, J., & Lennie, P. (1984). Chromatic mechanisms in lateral geniculate nucleus of macaque. *Journal of Physiology*, *357*(1), 241–265.

Hofer, H., Carroll, J., Neitz, M., Neitz, J., & Williams, D. R. (2003). Organization of the human trichromatic cone mosaic. *Journal of Neuroscience*, *44*(13), 1909.

Holtsmark, T. (1969). Colour discrimination and hue. *Nature*, *224*(5217), 366–367.

Jordan, G., Deeb, S. S., Bosten, J. M., & Mollon, J. D. (2010). The dimensionality of color vision in carriers of anomalous trichromacy. *Journal of Vision*, *8*(10), 1–19.

Koenderink, J. J., & Van Doorn, A. J. (2003). Perspectives on colour space. In R. Mausfeld & D. Heyer (Eds.), *Colour perception: Mind and the physical world* (pp. 1–56). Oxford: Oxford University Press.

Landa, E. R., & Fairchild, M. D. (2005). Charting color from the eye of the beholder. *American Scientist*, *93*(5), 436–443.

Laparra, V., Jiménez, S., Camps, G., & Malo, J. (2012). Nonlinearities and adaptation of color vision from sequential principal curves analysis. *Neural Computation*, *24*(10), 2751–2788.

Laparra, V., & Malo, J. (2015). Visual after effects and sensory nonlinearities from a single statistical framework. *Frontiers in Human Neuroscience*, *9*, 557.

Laparra, V., Muñoz, J., & Malo, J. (2010). Divisive normalization image quality metric revisited. *Journal of the Optical Society of America A*, *27*(6), 852–864.

Laughlin, S. B. (1981). A simple coding enhances a neuron's information capacity. *Zeitschrift für Naturforschung, 36*c, 910–912.

Laughlin, S. B. (1983). Matching coding to scenes to enhance efficiency. In O. J. Braddick & A. C. Sleigh (Eds.), *Physical and biological processing of images* (pp. 42–52). Berlin: Springer.

MacAdam, D. L. (1942). Visual sensitivities to color differences in daylight. *Journal of the Optical Society of America*, *32*(5), 247–274.

MacAdam, D. L. (1944). On the geometry of color space. *Journal of the Franklin Institute*, *238*(5), 195–201.

MacLeod, D. I. A. (2003). Colour discrimination, colour constancy, and natural scene statistics. In J. Mollon, J. Pokorny, & K. Knoblach (Eds.), *Normal and defective colour vision* (pp. 189–218). London: Oxford University Press.

MacLeod, D. I. A., & von der Twer, T. (2003). The pleistochrome: Optimal opponent codes for natural colours. In R. Mausfeld & D. Heyer (Eds.), *Colour perception: Mind and the physical world* Oxford: Oxford University Press.

Malacara, D. (2011). *Color vision and colorimetry: Theory and applications*. Bellingham, WA: SPIE.

Malo, J., & Laparra, V. (2010). Psychophysically tuned divisive normalization approximately factorizes the PDF of natural images. *Neural Computation*, *22*(12), 3179–3206.

Munsell, A. H. (1912). A pigment color system and notation. *American Journal of Psychology*, *23*(2), 236–244.

Pokorny, J., & Smith, V. C. (1970). Wavelength discrimination in the presence of added chromatic fields. *Journal of the Optical Society of America*, *60*(4), 562–569.

Roorda, A., & Williams, D. D. (1999). The arrangement of the three cone classes in the living human eye. *Nature*, *397*, 520–522.

Silberstein, L. (1943). Investigations on the intrinsic properties of the color domain. *Journal of the Optical Society of America*, *33*(1), 1–10.

Srinivasan, M. V., Laughlin, S. B., & Dubs, A. (1982). Predictive coding: A fresh view of inhibition in the retina. *Proceedings of the Royal Society of London B*, *216*(1205), 427–459.

Stockman, A., & Brainard, D. H. (2009). Color vision mechanisms. In M. Bass (Ed.), *Handbook of optics* (vol. 3, pp. 1–104). New York: McGraw-Hill.

von der Twer, T., & MacLeod, D. I. A. (2001). Optimal nonlinear codes for the perception of natural colours. *Network: Computation in Neural Systems*, *12*(3), 395–407.

Wright, W. D., & Pitt, F. H. G. (1934). Hue discrimination in normal colour vision. *Proceedings of the Physical Society*, *46*(3), 459–473.

Wyszecki, G., & Stiles, W. S. (2000). *Color science: Concepts and methods, quantitative data and formulae*. New York: Wiley Interscience.

Zhaoping, L., Geisler, W. S., & May, K. A. (2011). Human wavelength discrimination of monochromatic light explained by optimal wavelength decoding of light of unknown intensity. *PLoS One*, *6*(5), e19248.

Received July 31, 2017; accepted January 11, 2018.